Journal of Power Sources 219 (2012) 217–222

Contents lists available at SciVerse ScienceDirect

Journal of Power Sources

journal homepage: www.elsevier.com/locate/jpowsour

The importance of "going nano" for high power battery materials

Dominic Bresser [a], Elie Paillard [a,*], Mark Copley [b], Peter Bishop [b], Martin Winter [a], Stefano Passerini [a,*]

[a] Institute of Physical Chemistry & MEET Battery Research Centre, University of Muenster, Corrensstr. 28/30 & 46, 48149 Muenster, Germany
[b] Johnson Matthey Technology Centre, Blounts Court Road, Reading, Berkshire RG4 9NH, United Kingdom

HIGHLIGHTS

- Flame spray pyrolysis $Li_4Ti_5O_{12}$ nanoparticles were successfully synthesized.
- $Li_4Ti_5O_{12}$ nanoparticles show very reversible lithium insertion performance.
- Electrodes composed of $Li_4Ti_5O_{12}$ nanoparticles show superior rate performance (100 C).
- $Li_4Ti_5O_{12}$ electrodes offer a capacity retention of 94.8% after 1000 cycles at 10 C.

ARTICLE INFO

Article history:
Received 21 May 2012
Received in revised form
30 June 2012
Accepted 13 July 2012
Available online 24 July 2012

Keywords:
$Li_4Ti_5O_{12}$
LTO
Nanoparticles
Lithium-ion anode
Battery

ABSTRACT

The electrochemical performance of spinel $Li_4Ti_5O_{12}$ (LTO) nanoparticles synthesized by flame spray pyrolysis with an average diameter of approximately 20–30 nm is reported in this manuscript and compared with that of micro-sized LTO particles (1–2 μm) formed by a thermal post-treatment of the nanoparticles. The significantly advanced high rate capability of nano-sized LTO is evidenced by the results from the galvanostatic tests with applied current densities of up to 17.5 A g^{-1}, corresponding to a full (dis-)charge of the cell within less than 40 s. For nano-sized LTO, specific capacities of 115 and 70 mAh g^{-1} were obtained for applied rates of 10 C and 100 C, respectively, thus confirming the essential influence of particle size of lithium titanate on its high rate capability and practical power density. Moreover, a capacity retention of around 94.8% was observed after 1000 cycles at 10 C, presenting LTO nanoparticles synthesized by FSP as highly promising anode material for high power lithium-ion battery applications.

1. Introduction

Since lithium-ion batteries offer at the same time high energy and power densities, they are nowadays the leading battery technology in the field of portable electronics. Thus, they are also considered as most promising candidate for the realization of fully electric vehicles and by this allowing a fully greenhouse gas emission free future transportation system [1]. Current lithium-ion technology is mainly based on the utilization of graphite on the anode side due to its relatively high specific capacity (372 mAh g^{-1}) and a lithium (de-)intercalation potential close to that of the Li^+/Li redox couple, which result in a rather high energy density of the final lithium-ion cell [2]. However, with respect to large scale applications, for instance electric vehicles, not only the energy density provided by a system is of major importance but also its power density and, especially, safety. Hence, the major advantage of carbonaceous electrode materials, particularly graphite, which is the low lithium-ion (de-)intercalation potential, turns out as one of its major drawbacks. This low operation potential, being much beyond the electrochemical stability window of common organic electrolytes, does not only cause electrolyte decomposition, but furthermore entails the inherent risk of metallic lithium plating [2–4], thus, resulting in severe safety issues and limiting the possible use of these materials particularly in electric and hybrid electric vehicles.

Titanium based electrodes operate at rather high potentials versus Li^+/Li. Hence, there is an intrinsic limitation in terms of energy density for lithium-ion cells based on the utilization of these materials as anodes. Nevertheless, this drawback can be more than compensated by the low cost, ease of recyclability, inherent safety, resulting from the operation within the electrochemical stability window of common organic electrolytes, the lower reactivity in the fully lithiated state [5,6], and the enhanced power density of these materials. Recently, we have reported the utilization of anatase TiO_2

* Corresponding authors.
E-mail addresses: Elie.Paillard@uni-muenster.de (E. Paillard), Stefano.Passerini@uni-muenster.de (S. Passerini).

0378-7753/$ – see front matter © 2012 Elsevier B.V. All rights reserved.
http://dx.doi.org/10.1016/j.jpowsour.2012.07.035

nanorods embedded in carbonaceous percolating networks for high power applications [7].

Nevertheless, so far mostly $Li_4Ti_5O_{12}$ (LTO) based electrodes, reported as possible anode material for rechargeable lithium-ion batteries for the first time by Ferg et al. in 1994 [8], have been used for commercial applications [9]. Hence, LTO is currently considered as one of the most promising anode materials to replace graphite in lithium-ion cells for large scale applications, particularly in combination with high voltage cathodes as, for instance, $LiNi_{0.4}Mn_{1.6}O_4$, resulting in 3 V lithium-ion cells [10–12]. Due to a lithium (de-)insertion potential of around 1.55 V, the current issues in terms of safety as e.g., dendrite formation, lithium plating, and electrolyte decomposition can be avoided [8,13,14]. Furthermore, LTO offers an outstanding cycling stability due to negligible volume expansion upon (de-)lithiation ("zero-strain material") [14]. However, due to the rather high lithium (de-)insertion potential and the limited specific capacity of 175 mAh g^{-1} [14], high energy applications are not the first choice for the application of LTO based electrodes. Thus, current and future research on LTO mainly focuses on high power applications in which fast electrode charges and discharges are required. Since nanomaterials in general offer an increased electrode-electrolyte contact area and shorter diffusion pathways for electrons as well as lithium ions [6,15], reducing the particle size is a promising strategy to enhance the high rate capability of LTO based electrodes [16–18]. In order to confirm this general assumption, herein nanoparticulate LTO has been synthesized by flame spray pyrolysis (FSP), which is considered a highly attractive method to produce nanosized particles of a variety of materials with tailored functionalities on a large scale [19,20]. The performance of the LTO nanoparticles is compared to that of micro-sized LTO – resulting from a thermal post treatment of nanoparticulate LTO – by performing galvanostatic cycling at elevated current densities to investigate the high rate capability or, in other words, the power density obtainable for LTO anode materials in dependence on its particle size.

2. Experimental

2.1. LTO synthesis, morphological, and structural characterization

Nano-sized LTO (LTO_{nano}) has been synthesized by flame spray pyrolysis (FSP). Subsequent thermal treatment at 800 °C under air in order to remove phase impurities resulted in particle growth with a particle diameter in the range of several micrometers (LTO_{micro}). Characterization of the morphology and particle size have been carried out by means of powder X-ray diffraction (XRD) on a Bruker D8 Advance (Cu-Kα radiation, $\lambda = 0.154$ nm) and high resolution scanning electron microscopy (HRSEM) using a ZEISS Auriga® microscope. The Brunauer–Emmett–Teller (BET) surface area has been determined by nitrogen adsorption measurements utilizing an ASAP 2020 (Accelerated Surface Area and Porosimetry Analyzer, MICROMERITICS).

2.2. Electrode preparation

LTO_{micro} and LTO_{nano} have been mixed with poly(vinylidendifluoride)-co(hexafluoropropylene) (PVDF-HFP) copolymer (Kynarflex 2801, ARKEMA) and Cnergy SuperC65® conductive carbon (TIMCAL) as the binder and conductive agent, respectively. *N*-methylpyrrolidone (ALDRICH) was used as the solvent. The mixture was subsequently homogenized by using a planetary ball mill (Vario-Planetary Mill Pulverisette 4, FRITSCH) set at 800 rpm for 2 h. The resulting slurries were then casted on dendritic copper foil (SCHLENK) by using a laboratory doctor blade with a wet film thickness of 120 μm. The electrodes were subsequently dried in air for 2 h at 80 °C and 12 h at RT. Disk electrodes (12 mm diameter) were punched out of the electrode tapes and dried for 12 h at 120 °C under vacuum. The active material mass loading was comprised between 2.6 and 2.8 mg cm^{-2} for the micro-sized and between 1.5 and 1.7 mg cm^{-2} for the nano-sized LTO. The final weight composition of the LTO_{micro} and LTO_{nano} electrodes was 78:12:10 and 70:15:15, respectively, in terms of active material, conductive additive, and binder.

2.3. Electrochemical characterization

Galvanostatic cycling has been performed at room temperature utilizing three-electrode Swagelok™-type cells, with lithium metal foil (CHEMETALL, lithium battery grade) as counter and reference electrodes. Cells were assembled in an MBraun glove box with oxygen and water contents below 0.5 ppm. A stack of polypropylene fleeces (Freudenberg FS 2226) drenched with a 1 M solution of $LiPF_6$ in a 3:7 volume ratio of ethylene carbonate (EC) and diethyl carbonate (DEC) (UBE) was used as electrolyte. All potential values reported in this manuscript refer to the Li^+/Li reference couple. The lower and upper cut-off potentials were set to 1.2 and 2.2 V, respectively, while a C-rate of 1 C corresponds to an applied current density of 175 mA g^{-1}.

3. Results and discussion

Nanosized LTO synthesized by FSP showed a very uniform particle size distribution, approximately between 20 and 30 nm (Fig. 1a and b), and a BET surface area of around 91.7 m^2 g^{-1}. According to Kavan et al. [18] LTO samples having a specific surface area of 20–100 m^2 g^{-1} are considered as preferable for application as lithium-ion anodes. Moreover, FSP as synthesis method allows the production of nanoparticles on a large scale and competitive price. Hence, nanoparticles produced by means of FSP can be considered as highly promising for commercialization. However, beside the main fraction of spinel $Li_4Ti_5O_{12}$ (JCPDS 00-049-0207, *Fd*-3*m* space group) several phase impurities as rutile and anatase TiO_2 as well as another lithium titanate phase could be detected by means of XRD analysis (Fig. 2a). Thus, first attempts to reduce the amount of phase impurities by subsequent thermal treatment resulted in rapid particle growth as it is clearly indicated by SEM observation (Fig. 1c), as well as XRD, increased peak intensity and reduced peak broadening (Fig. 2b), and BET, a decreased surface area by a factor of almost 100 (to about 1 m^2 g^{-1}) characterizations. Nevertheless, the amount of phase impurities was successfully reduced, as can be seen in Fig. 2b), confirming the results reported by Ernst et al. [21].

The differences in particle size of the two samples offered the opportunity to investigate the influence of the particle size on the electrochemical performance of LTO powders synthesized by FSP. Thus, galvanostatic cycling was performed for electrodes based on these two materials. The corresponding voltage profiles for the first cycle of LTO_{micro} and LTO_{nano} electrodes are shown in Fig. 3a) and b), respectively. Significantly increased solid solution domains, before and after the voltage plateau for the discharge (charge) process, are observed for LTO_{nano}. Such variations in the extension of the solid solution phases, already reported for anatase TiO_2 nanorods [7] as well as for high surface area LTO [22], are likely related to changes in the surface and interface energies, as reported by Wagemaker et al. [23], which impact increases for decreasing particle size and increasing surface area. Nevertheless, LTO_{micro} showed first cycle reversible capacity of 145 mAh g^{-1} and coulombic efficiency of 94.7%, which were substantially higher than those observed for LTO_{nano}, respectively, 131 mAh g^{-1} and 77.2%. Jiang et al. [5] have shown that lithiated LTO reacts with $LiPF_6$-EC/DEC electrolytes, to

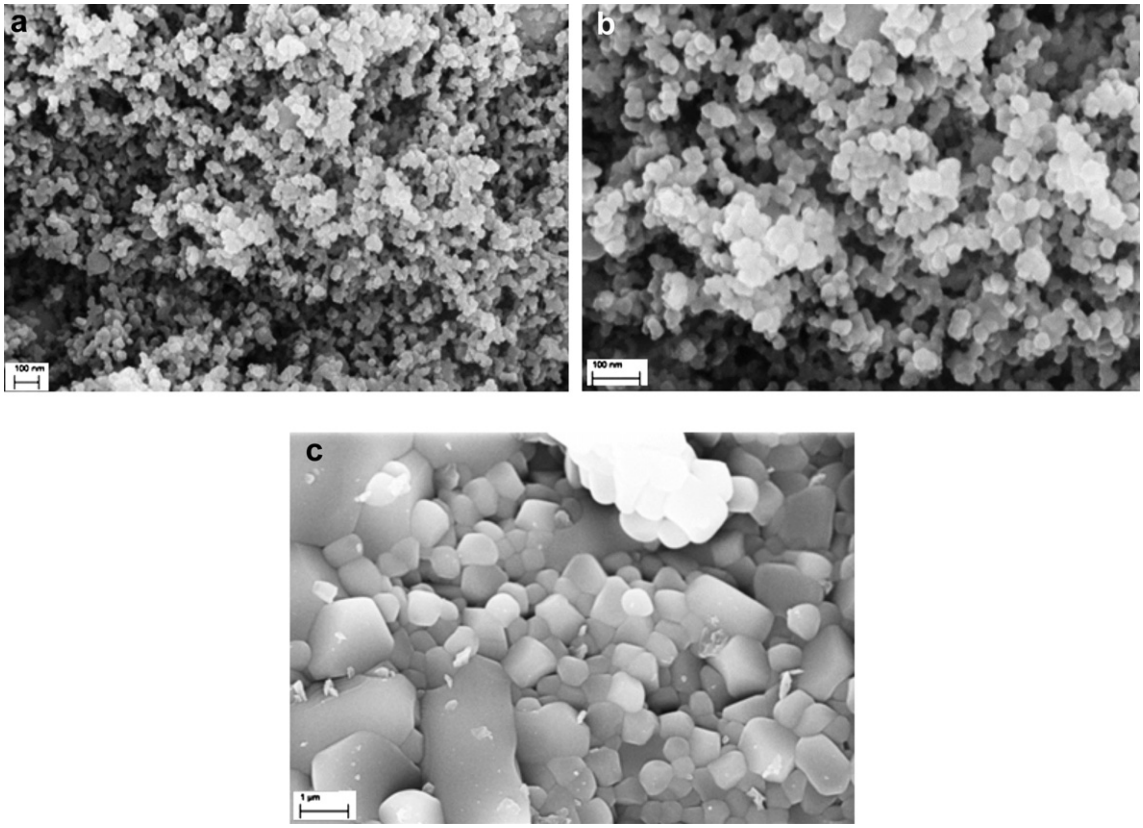

Fig. 1. HRSEM images of a LTO_{nano} powder with different magnifications (panels a and b). HRSEM image of LTO_{micro} as obtained after thermal treatment of LTO_{nano} (panel c).

form LiF, Li_2CO_3, and TiO_2. Since this reaction takes place at the surface of the particles, increasing the specific surface area of LTO powders naturally results in an increased irreversibility upon initial cycles. Moreover, the relatively higher ratio of phase impurities for LTO_{nano} might have a significant influence on the 1st cycle coulombic efficiency. Particularly, for rutile TiO_2, being the most pronounced phase impurity, a rather high irreversible capacity loss has been reported for the first cycle, which likely has its origin within irreversible structural changes upon initial lithiation [24–26]. However, future studies on optimized samples might offer further insight on the influence of the other phases on this specific issue as well as on the overall electrochemical performance.

Increasing the C rate stepwise to 1 C, 2 C, 5 C, 10 C, 20 C, 30 C, 40 C, 50 C, 60 C, 70 C, 80 C, 90 C, and finally 100 C illustrates the distinct advantage of particles with an average diameter of around 20–30 nm (Fig. 3c and d). In fact, LTO_{micro} capacity (Fig. 3c) drops rather quickly to a specific capacity of only 1.5 mAh g^{-1} for an applied current density of 17.5 A g^{-1}, corresponding to a C rate of 100 C. Although the voltage plateau, corresponding to the two phase equilibrium of lithium-poor spinel $Li_{4/3}Ti_{5/3}O_4$ and lithium-

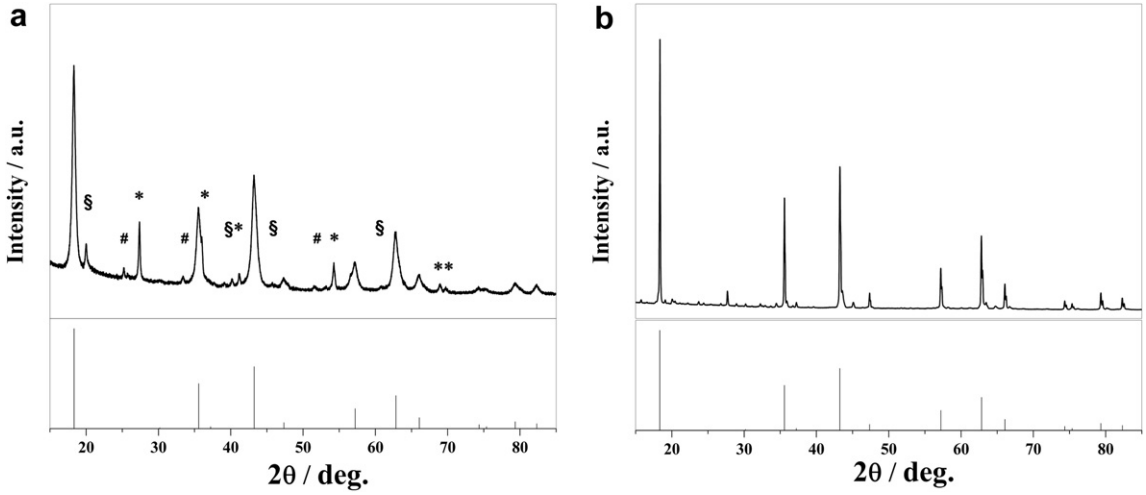

Fig. 2. XRD pattern of LTO_{nano} (panel a) and LTO_{micro} (panel b). For comparison purposes, the JCPDS reference 00-049-0207 for spinel LTO is shown in the bottom of each panel. Additional peaks corresponding to rutile TiO_2, anatase TiO_2, and $Li_3Ti_3O_7$ are marked by *, #, and §, respectively.

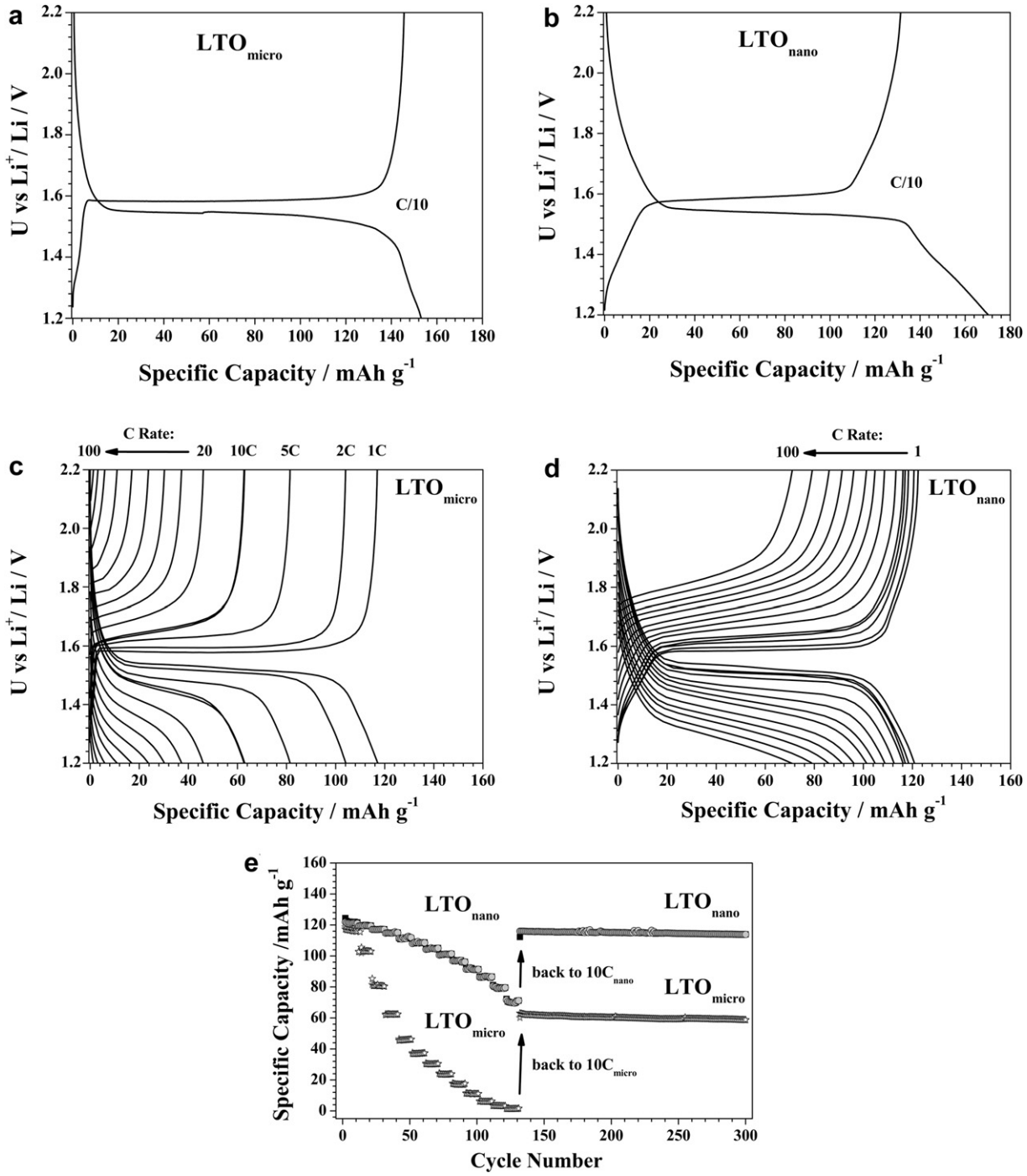

Fig. 3. Performance of LTO_{micro} and LTO_{nano} electrodes upon continuous galvanostatic charge discharge tests at elevated C rates. 1st cycle C/10. Subsequently, series of 10 cycles were performed at rate of 1 C, 2 C, 5 C, 10 C, 20 C, 30 C, 40 C, 50 C, 60 C, 70 C, 80 C, 90 C, and 100 C. Finally, the electrodes were subjected to additional 170 cycles at 10 C rate. Cut-off potentials: 1.2 V–2.2 V. Voltage profile *vs*. specific capacity during the 1st cycle of LTO_{micro} (panel a) and LTO_{nano} (panel b) electrodes. Voltage profiles *vs*. specific capacity for the different C rates of LTO_{micro} (panel c) and LTO_{nano} (panel d) electrodes. The corresponding specific capacities of these electrodes are also compared (panel e; 1st cycle not shown).

rich rock-salt $Li_{7/3}Ti_{5/3}O_4$ upon lithium (de-)insertion [22,27] is rather well preserved up to 10 C, the increasing overpotential within the cell leads to a steadily decreasing specific capacity. Such an increase in overpotential can also be observed for LTO_{nano}, but much less pronounced (Fig. 3d). In fact, a rather slowly but constantly dropping IR (internal resistance) within the LTO_{nano} cells can be observed, resulting in a highly stable capacity retention even for elevated C-rates as high as 100 C. Comparing the electrochemical performance in terms of specific capacity *vs*. cycle number (Fig. 3e) illustrates further these significant differences. While the specific capacity of LTO_{nano} decreases only stepwise upon applying elevated current densities that of LTO_{micro} drops rather rapidly. Hence, it can be clearly seen that decreasing the particle size to the nanoscale, by this increasing the electrolyte–electrode contact area and decreasing the lithium-ion and electron diffusion pathway, finally results in a much improved power density.

Additionally, LTO nanoparticles are converted much faster into the highly conductive, fully lithiated $Li_7Ti_5O_{12}$ phase [28], which is very likely to contribute to its excellent high rate capability. However, remarkably for both electrodes, highly stable capacity retention can be obtained after decreasing the applied current density to 1.75 A g^{-1} or a corresponding C-rate of 10 C. It should be noted at this point, that the improved electrochemical performance of LTO_{nano} relatively to LTO_{micro} might also be partially influenced by the different mass loading of the prepared electrodes, resulting in an applied current density of around 28 and 47 mA cm^{-2} for LTO_{nano} and LTO_{micro}, respectively, each corresponding to 100 C. This different mass loading is a result of a different density of the slurry upon electrode preparation as well as the finally dried active material casted on the current collector by applying the same wet film thickness. However, the differences in electrochemical performance cannot be explained by the mass loading difference, particularly since for LTO_{nano}, already for rather low C-rates of 2 and 5 C, a significantly enhanced high rate capability is observed.

In Fig. 4a) the long-term cycling stability of LTO_{nano} electrodes at 10 C is shown. The rather high irreversibility within the first formation cycle at C/10 has already been discussed previously. On subsequent cycles, however, these electrodes offer highly stable capacity retention for more than 1000 cycles with a total capacity loss of only 5.2% and a coulombic efficiency of more than 99.9% upon subsequent continuous galvanostatic charge–discharge tests.

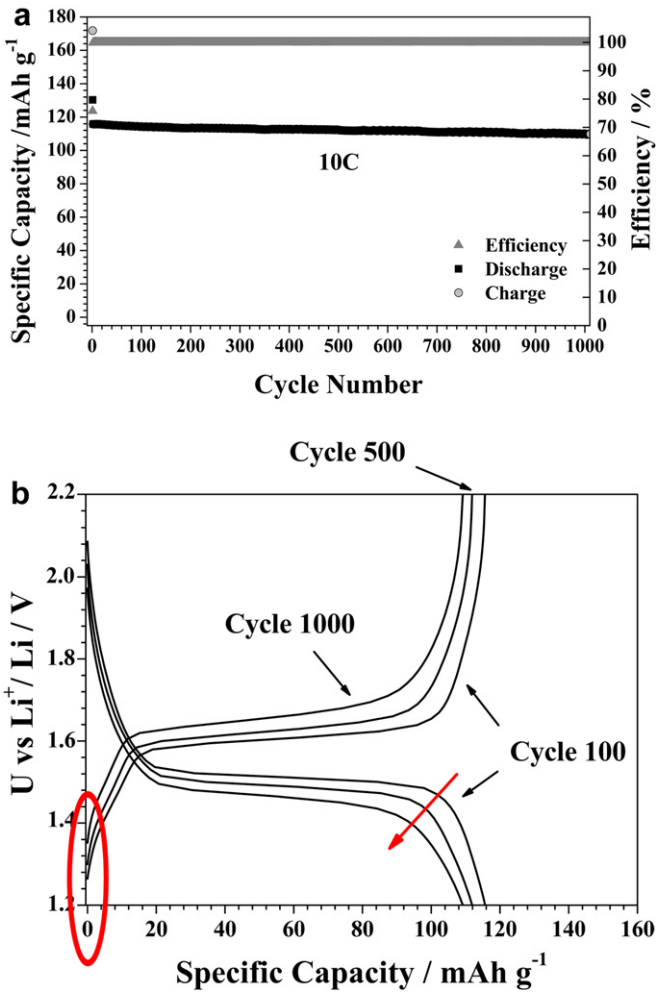

Fig. 4. Galvanostatic charge discharge tests at 10 C rate of a LTO_{nano} electrode. 1st cycle C/10. Cut-off potentials: 1.2 V–2.2 V. Specific capacity vs. cycle number for all cycles (panel a). Voltage profile vs. specific capacity for the cycles 100, 500, and 1000 (panel b).

As can be seen in Fig. 4b), the reason for this very little capacity loss after 1000 cycles is related firstly, to a shortening of the main voltage plateau. Accordingly, the voltage profile after the main plateau becomes less steep (marked by the red arrow), indicating slight structural changes within the LTO host lattice upon continuous (de-)lithiation and an increasing solid solution domain. Secondly, an increase of the IR drop upon continuous galvanostatic cycling appears, as indicated by the red marking, further contributing to the observed slight decrease in capacity retention. Hence, further improvement of the material will mainly focus on the improvement of the electronic conductivity within the final electrode as well as the synthesis parameters in order to obtain single-phase LTO, offering higher specific capacities at low C-rate. A subsequent comparison might also enlighten a possible influence of the present phase impurities on the electrochemical performance of the investigated LTO_{nano}. Nevertheless, the obtained results have shown a great improvement of electrochemical performance, particularly in terms of high rate capability, compared to earlier reported results on LTO nanoparticles obtained by FSP [29–31], and to the best of our knowledge so far only few results have been reported showing comparable power performance as well as cycling stability [17,32–34].

4. Conclusion

Lithium (de-)insertion in micro- and nano-sized $Li_4Ti_5O_{12}$ synthesized by means of FSP has been comparatively investigated by applying elevated current densities of up to 17.5 A g^{-1}, corresponding to a (dis-)charge rate of 100 C. Charging and discharging micro- and nano-sized LTO in less than 40 s revealed in reversible specific capacities of 1.5 and 70 mAh g^{-1}, respectively. Based on these results it has been shown that a reduction of the particle size from several micrometers to the nanometer scale results in a significantly enhanced high rate capability of LTO based electrodes. Furthermore, LTO_{nano} electrodes have shown coulombic efficiencies of more than 99.9%, resulting in advanced capacity retention and cycling stability for more than 1000 cycles at a C-rate of 10 C.

Thus, LTO nanoparticles can be considered as highly promising anode material for the realization of low cost, safe, and environmentally friendly high power lithium-ion batteries and supercapacitors for large-scale applications, as for instance electric vehicles.

Acknowledgment

Financial support from the European Commission within the ORION project (229036) under the Seventh Framework Programme (7th FWP) is gratefully acknowledged. Furthermore, the authors want to thank Mr. Steffen Krueger for performing SEM analysis.

References

[1] M.Z. Jacobson, M.A. Delucchi, Scientific American 301 (2009) 58–65.
[2] R. Yazami, Electrochimica Acta 45 (1999) 87–97.
[3] S. Flandrois, B. Simon, Carbon (American Carbon Committee) 37 (1999) 165–180.
[4] E. Peled, Journal of the Electrochemical Society 126 (1979) 2047–2051.
[5] J. Jiang, J. Chen, J.R. Dahn, Journal of the Electrochemical Society 151 (2004) A2082–A2087.
[6] A.S. Aricò, P. Bruce, B. Scrosati, J.M. Tarascon, W. van Schalkwijk, Nature Materials 4 (2005) 366–377.
[7] D. Bresser, E. Paillard, E. Binetti, S. Krueger, M. Striccoli, M. Winter, S. Passerini, Journal of Power Sources 206 (2012) 301–309.
[8] E. Ferg, R.J. Gummow, A. de Kock, M.M. Thackeray, Journal of the Electrochemical Society 141 (1994) L147–L150.
[9] B. Scrosati, J. Garche, Journal of Power Sources 195 (2010) 2419–2430.

[10] S. Patoux, L. Sannier, H. Lignier, Y. Reynier, C. Bourbon, S. Jouanneau, F. Le Cras, S. Martinet, Electrochimica Acta 53 (2008) 4137–4145.
[11] S. Patoux, L. Daniel, C. Bourbon, H. Lignier, C. Pagano, F. Le Cras, S. Jouanneau, S. Martinet, Journal of Power Sources 189 (2009) 344–352.
[12] K. Ariyoshi, T. Ohzuku, Journal of Power Sources 174 (2007) 1258–1262.
[13] K.M. Colbow, J.R. Dahn, R.R. Haering, Journal of Power Sources 26 (1989) 397–402.
[14] T. Ohzuku, A. Ueda, N. Yamamoto, Journal of the Electrochemical Society 142 (1995) 1431–1435.
[15] M. Armand, J.-M. Tarascon, Nature 451 (2008) 652–657.
[16] N. Zhang, Z. Liu, T. Yang, C. Liao, Z. Wang, K. Sun, Electrochemistry Communications 13 (2011) 654–656.
[17] A.S. Prakash, P. Manikandan, K. Ramesha, M. Sathiya, J.-M. Tarascon, A.K. Shukla, Chemistry of Materials 22 (2010) 2857–2863.
[18] L. Kavan, J. Prochazka, T.M. Spitler, M. Kalbac, M. Zukalova, T. Drezen, M. Gratzel, Journal of the Electrochemical Society 150 (2003) A1000–A1007.
[19] R. Mueller, L. Mädler, S.E. Pratsinis, Chemical Engineering Science 58 (2003) 1969–1976.
[20] W.Y. Teoh, R. Amal, L. Madler, Nanoscale 2 (2010) 1324–1347.
[21] F.O. Ernst, H.K. Kammler, A. Roessler, S.E. Pratsinis, W.J. Stark, J. Ufheil, P. Novák, Materials Chemistry and Physics 101 (2007) 372–378.
[22] S. Scharner, W. Weppner, P. Schmid-Beurmann, Journal of the Electrochemical Society 146 (1999) 857–861.
[23] M. Wagemaker, F.M. Mulder, A. Van der Ven, Advanced Materials 21 (2009) 2703–2709.
[24] D. Dambournet, I. Belharouak, K. Amine, Chemistry of Materials 22 (2009) 1173–1179.
[25] Y.-S. Hu, L. Kienle, Y.-G. Guo, J. Maier, Advanced Materials 18 (2006) 1421.
[26] W.J.H. Borghols, M. Wagemaker, U. Lafont, E.M. Kelder, F.M. Mulder, Chemistry of Materials 20 (2008) 2949–2955.
[27] L. Aldon, P. Kubiak, M. Womes, J.C. Jumas, J. Olivier-Fourcade, J.L. Tirado, J.I. Corredor, C. Pérez Vicente, Chemistry of Materials 16 (2004) 5721–5725.
[28] M. Wagemaker, D.R. Simon, E.M. Kelder, J. Schoonman, C. Ringpfeil, U. Haake, D. Lützenkirchen-Hecht, R. Frahm, F.M. Mulder, Advanced Materials 18 (2006) 3169–3173.
[29] S.H. Ju, Y.C. Kang, Journal of Physics and Chemistry of Solids 70 (2009) 40–44.
[30] S.H. Ju, Y.C. Kang, Journal of Power Sources 189 (2009) 185–190.
[31] S.H. Ju, Y.C. Kang, Journal of Alloys and Compounds 506 (2010) 913–916.
[32] E. Kang, Y.S. Jung, G.-H. Kim, J. Chun, U. Wiesner, A.C. Dillon, J.K. Kim, J. Lee, Advanced Functional Materials 21 (2011) 4349–4357.
[33] K. Naoi, S. Ishimoto, Y. Isobe, S. Aoyagi, Journal of Power Sources 195 (2010) 6250–6254.
[34] K. Naoi, Fuel Cells 10 (2010) 825–833.